Ultrafast nonequilibrium Fourier-transform two-dimensional infrared spectroscopy

Carlos R. Baiz, Matthew J. Nee, Robert McCanne, and Kevin J. Kubarych*

Department of Chemistry, University of Michigan, 930 North University Avenue, Ann Arbor, Michigan 48109, USA
**Corresponding author: kubarych@umich.edu*

Received July 28, 2008; revised September 18, 2008; accepted September 23, 2008;
posted October 7, 2008 (Doc. ID 99439); published October 29, 2008

We present what we believe to be the first implementation of nonequilibrium two-dimensional IR spectroscopy (2DIR) combining electronic excitation within the Fourier transform (FT) approach. Nonequilibrium 2DIR spectra of $Mn_2(CO)_{10}$ and its photoproducts are obtained in two modalities: photoexcitation at 400 nm, either before a 2DIR probe or during the waiting time of the FT 2DIR measurement. Extending FT 2DIR to nonequilibrium systems offers insight into complex condensed-phase reaction dynamics. © 2008 Optical Society of America

OCIS codes: 320.7100, 300.6340.

Two-dimensional IR spectroscopy (2DIR) provides experimental access to ultrafast molecular dynamics by spreading congested condensed phase spectra into two frequency axes [1,2]. 2DIR measurements also report couplings between vibrational transitions, intramolecular vibrational redistribution (IVR), and vibrational population relaxation, as well as spectral diffusion due to evolving solvent environments. To date, the bulk of 2DIR experiment and theory has focused on systems in electronic ground states. Bredenbeck *et al.* [3] and Hamm *et al.* [4] have developed nonequilibrium variants of 2DIR by introducing an optical perturbation before or during the 2DIR measurement to study photoswitchable peptides [5], disulfide bond breaking [6], and metal-to-ligand charge transfer [7]. In addition, Chung *et al.* [8] have used Fourier transform (FT) 2DIR as a probe of protein unfolding dynamics. We report here the introduction of transient photochemistry to the background-free FT implementation of 2DIR, which offers advantages in sensitivity and independent temporal and spectral resolution [9]. Further, we have combined transient 2DIR spectroscopy with the chirped-pulse upconversion detection technique [10,11]. In this Letter nonequilibrium 2DIR describes two different techniques: triggered-exchange 2DIR (TE-2DIR) and transient-2DIR (t-2DIR). TE-2DIR provides vibrational mode correlation in optically triggered processes by mapping reactant vibrations to product vibrations, thus avoiding ambiguities associated with one-dimensional transient absorption methods [3]. Transient-2DIR extends to transient species the structurally sensitive information inherent to 2DIR, such as normal-mode coupling and vibrational energy transfer rates with a temporal dynamic range spanning multiple time scales. Previous TE-2DIR experiments used a narrowband-pump–broadband-probe approach, with the IR pump spectral resolution determined by the bandwidth of a tunable Fabry–Perot etalon—typically $5-10\ cm^{-1}$—resulting in IR pump pulses of several picoseconds duration, thus linking temporal and spectral resolution [9]. A key advantage of the FT implementation of TE-2DIR is that all pulses are ultrashort and the spectral resolution is limited by the maximum coherence time delay. Since the second field–matter interaction is with an ultrashort pulse, smaller waiting time delays can be probed, and the UV pulse initiating the chemical reaction can excite the system before appreciable IVR has taken place. This is significant when IVR is fast (<1 to 2 ps), as the excitation energy rapidly randomizes among the modes and excitation-detection frequency correlation is rapidly lost [12,13]. A disadvantage of FT 2DIR, however, lies in the technical difficulty of implementing the technique as well as the higher demand for phase stability. Combining the structural specificity and femtosecond time resolution inherent to FT 2DIR with UV photoexcitation, these techniques offer valuable insight into condensed-phase photochemistry.

The principles of 2DIR spectroscopy have been described in detail elsewhere [2]. Briefly, a 2DIR spectrum is obtained by applying three femtosecond IR pulses with wave vectors $\mathbf{k}_1$, $\mathbf{k}_2$, and $\mathbf{k}_3$, separated by time delays t_1 and t_2, producing a signal in a phase-matched background-free direction [Fig. 1(a)]. The electric field is recovered by interferometric superposition with a local oscillator in a spectrometer. In TE-2DIR, after vibrational labeling by the first two IR pulses, an additional pulse is applied to trigger a chemical process; the third pulse then probes the transient photoproducts, which are correlated to the

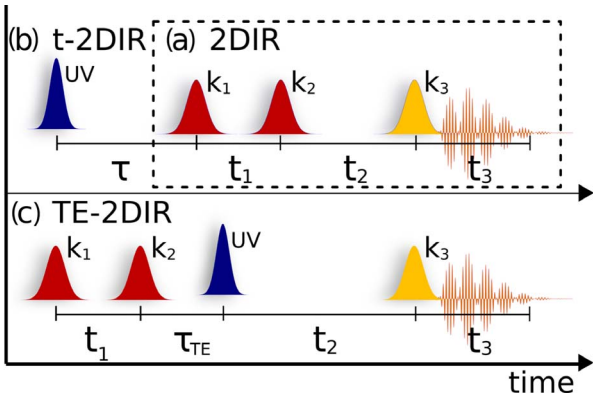

Fig. 1. (Color online) Fourier-transform (a) 2DIR, (b) t-2DIR, and (c) TE-2DIR pulse sequences. Red pulses represent $\mathbf{k}_1$ and $\mathbf{k}_2$, yellow represents $\mathbf{k}_3$, the radiated signal is shown in orange, and UV pulses are shown in blue.

0146-9592/08/212533-3/$15.00

initially excited reactant frequencies [Fig. 1(c)]. A t-2DIR spectrum is measured by applying the excitation pulse before the three IR pulses, thus obtaining a full 2D correlation spectrum of the transient species [Fig. 1(b)]. In this Letter we describe the optical setup (Fig. 2) used to obtain nonequilibrium 2DIR of $Mn_2(CO)_{10}$ and its photoproducts following UV excitation.

The 2DIR spectrometer used here has been described in detail elsewhere [11]. Briefly, 1 mJ of the 2 mJ output of a regeneratively amplified Ti:sapphire laser, centered at 800 nm with a 1 kHz repetition rate, generates near-IR pulses using β-barium borate (BBO) in a dual optical parametric amplifier (OPA), which is then used to generate two mid-IR pulses (3 μJ, 100 fs), centered at 2000 cm^{-1} with ~100 cm^{-1} FWHM bandwidth, by difference-frequency generation (DFG) in separate 1 mm GaSe crystals. The first IR beam is split into $\mathbf{k}_1$ and $\mathbf{k}_2$, and the second IR beam is split into $\mathbf{k}_3$, tracer, and local oscillator (Fig. 2). The beams are aligned in a box geometry, and the rephasing signal is measured in the $\mathbf{k}_s=-\mathbf{k}_1+\mathbf{k}_2+\mathbf{k}_3$ direction. The signal and reference local oscillator are upconverted by sum-frequency generation in a 0.5 mm $MgO:LiNbO_3$ crystal using a 45 μJ highly chirped pulse centered at 800 nm derived from the Ti:sapphire amplifier before compression [11]. The upconverted light is dispersed and detected with a 1340×100 pixel silicon CCD detector whose 20 active rows are vertically binned before readout, enabling single-shot detection at 1 kHz. To record a 2DIR spectrum for a given waiting time (t_2), the first time delay (t_1) is scanned continuously, and the heterodyned spectra along with the corresponding motor positions are collected synchronized to the laser. Rephasing 2DIR spectra require less than 8 s of total data acquisition time for ~16 ps of maximum t_1 delay, yielding a FT resolution of 2 cm^{-1}.

UV pulses centered at 400 nm (>30 μJ, ~100 fs) are generated by frequency doubling ~200 μJ of the amplifier output in a 0.4 mm BBO crystal. The UV beam is mechanically chopped to 250 Hz (25% duty cycle). Alignment of the UV beam is optimized by maximizing the contrast (pump on versus pump off) of the dispersed vibrational echo [(DVE), $t_1=t_2=0$] signal. Following alignment, the UV power is adjusted such that the bleach is <25% of the total DVE signal intensity, corresponding to 15–20 μJ of UV focused to a spot size of 300 μm FWHM. The UV–IR time overlap is also set using the DVE signal; $\tau=0$ is determined by scanning the UV pulse until the DVE bleaches decrease to 50% of the maximum value. A gravity-driven wire-guided liquid jet provides excellent film stability with a film thickness of approximately 200 μm, and an adequate linear flow refreshes the sample between laser shots [14]. The jet minimizes UV–IR temporal walk-off while reducing nonresonant signal contributions. Because the reference beam is routed around the sample (Fig. 2), film stability is critical for maintaining a constant relative phase between the signal and reference. Film fluctuations measured by fringe-tracking interferometry were found to have <60 nm rms deviations. Although the film profile introduces small lensing effects, proper focusing and alignment of the beams minimizes these effects on the 2D signal. The collected data set contains both pumped (pump on) and unpumped (pump off) ω_3 spectra as a function of t_1. After deinterlacing (Fig. 3), the pumped and unpumped data sets are Fourier transformed separately. Difference 2D spectra are obtained by subtracting the unpumped from the pumped absolute-value rephasing 2DIR spectra. The 25% chopper duty cycle provides three unpumped spectra for every pumped spectrum corresponding to 1, 2, and 3 ms sample refresh times. Proper flow rate was verified by comparing the difference spectra at the different refresh times.

The described setup has enabled us to measure TE-2DIR and t-2DIR spectra of $Mn_2(CO)_{10}$ in cyclohexane at 6 mM concentration, where excitation at 400 nm primarily cleaves the Mn–Mn bond [15], yielding two $Mn_2(CO)_5$. $Mn_2(CO)_{10}$, whose 2DIR

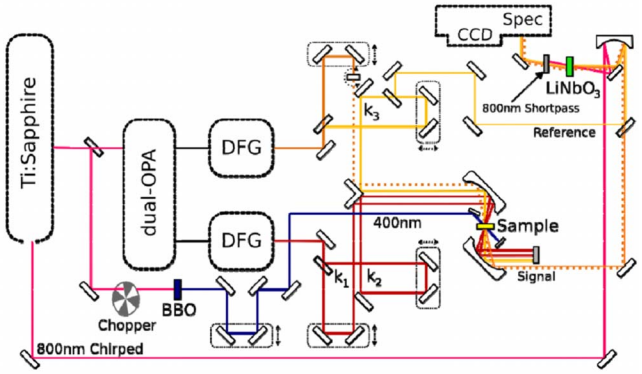

Fig. 2. (Color online) Nonequilibrium 2DIR spectrometer. The IR and UV beams are color coded according to the pulse sequences in Fig. 1. The dotted beam represents the tracer used for alignment and one-dimensional transient absorption measurements.

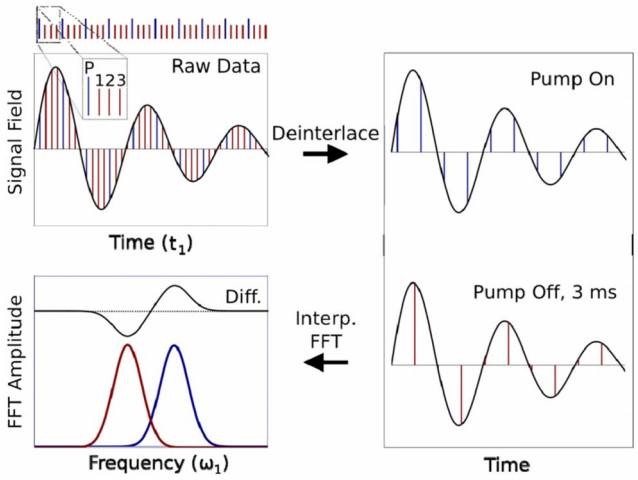

Fig. 3. (Color online) Schematic representation of the 2D data analysis process with a 25% chopper duty time. The two sets of data (with and without UV pump) are collected simultaneously. After deinterlacing the two sets are interpolated to uniform time points and Fourier transformed separately; the final difference spectrum is computed in the frequency domain.

spectrum has been reported previously [11,13], exhibits three absorption peaks 1983, 2013, and 2045 cm^{-1} and one main photoproduct band centered at 1982 cm^{-1}.

The TE-2DIR spectrum at $\tau_{TE}=1$ ps, $t_2=25$ ps [Fig. 4(a)] shows a positive peak at $\omega_1=2013$ cm^{-1}, $\omega_3=1982$ cm^{-1}, indicating a correlation between the 2013 cm^{-1} mode in $Mn_2(CO)_{10}$ and the 1982 cm^{-1} mode in $Mn_2(CO)_5$. The t-2DIR spectrum at $\tau=25$ ps, $t_2=1$ ps [Fig. 4(b)] shows a dominant feature centered around $\omega_1=1982$ cm^{-1}, $\omega_3=1982$ cm^{-1}, corresponding to the photoproduct. The broadness of this feature indicates that 25 ps after photolysis, the product molecules remain vibrationally hot, in agreement with previous transient UV pump-IR probe experiments [15]. The difference in relative amplitudes of the transient features in TE-2DIR and t-2DIR is attributed to different overlap with the IR pulse envelopes,

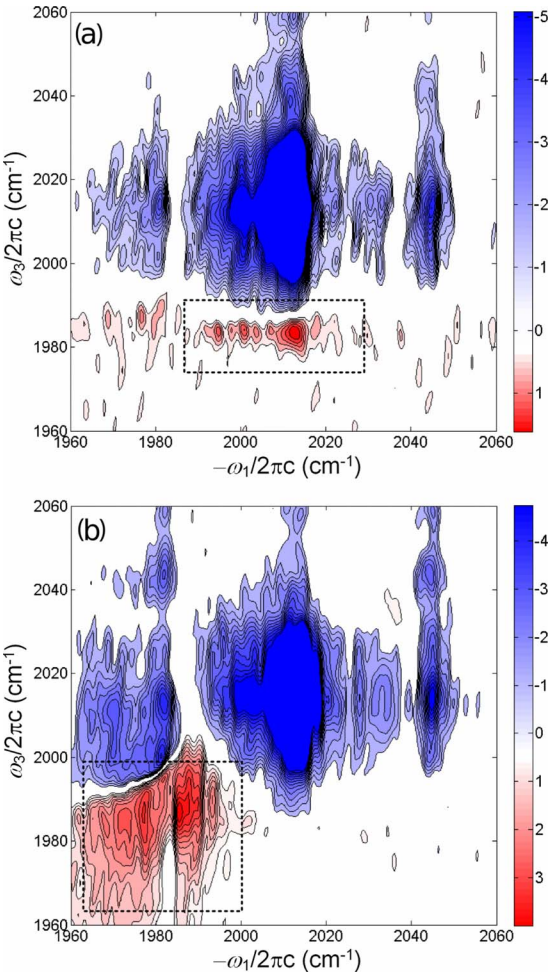

Fig. 4. (Color online) (a) Triggered-exchange 2DIR spectrum at $\tau_{TE}=1$ ps, $t_2=25$ ps. (b) Transient 2DIR spectrum of $Mn_2(CO)_{10}$ at $\tau=25$ ps, $t_2=1$ ps. Negative features [unboxed (blue online)] arise from the depletion of ground-state reactant molecules, while positive features [boxed (red online)] are due to nonequilibrium photoproducts. Contours smaller than 2% and larger than 30% of the maximum amplitude are omitted for clarity. The spectra are not corrected for the amplitude envelope of the mid-IR pulses.

spectral overlap with the parent bleaches, as well as differences in rotational diffusion and differences in oscillator strength. Low-frequency diagonal and off-diagonal bleaches are suppressed by tuning the mid-IR pump pulses to the high-frequency region of the spectrum so as to minimize the amplitude and 2D line shape distortion of the transient features due to spectral overlap.

$Mn_2(CO)_{10}$ presents a useful model system owing to its strong carbonyl stretching modes, rich vibrational level structure, and well-defined photoproduct. An attractive feature of t-2DIR is that despite spectral overlap with the parent molecule, the product spectrum can still be easily separated. Additionally, since the equilibrium dynamics of $Mn_2(CO)_{10}$ can be determined by 2DIR, the photoproduct contribution can be isolated—a capability unavailable in conventional transient absorption spectroscopy. A full characterization of the photochemistry of $Mn_2(CO)_{10}$, including reaction pathways, vibrational and electronic relaxation, as well as geminate rebinding ratios, can be investigated with nonequilibrium 2DIR and will be reported elsewhere. Further enhancements of the technique will include transient differential absorptive 2D spectra by recording both rephasing and nonrephasing signals, using the unpumped data for phasing. This is a general technique and can be used to study a wide range of photochemical processes with femtosecond time resolution and spectral resolution limited only by the molecular transitions.

We acknowledge support from the ACS Petroleum Research Fund and the National Science Foundation (NSF).

References

1. P. Hamm, M. H. Lim, and R. M. Hochstrasser, J. Phys. Chem. B **102**, 6123 (1998).
2. M. H. Cho, Chem. Rev. **108**, 1331 (2008).
3. J. Bredenbeck, J. Helbing, C. Kolano, and P. Hamm, ChemPhysChem **8**, 1747 (2007).
4. P. Hamm, J. Helbing, and J. Bredenbeck, Annu. Rev. Phys. Chem. **59**, 291 (2008).
5. C. Kolano, J. Helbing, M. Kozinski, W. Sander, and P. Hamm, Nature **444**, 469 (2006).
6. C. Kolano, J. Helbing, G. Bucher, W. Sander, and P. Hamm, J. Phys. Chem. B **111**, 11297 (2007).
7. J. Bredenbeck, J. Helbing, and P. Hamm, J. Am. Chem. Soc. **126**, 990 (2004).
8. H. S. Chung, Z. Ganim, K. C. Jones, and A. Tokmakoff, Proc. Natl. Acad. Sci. USA **104**, 14237 (2007).
9. V. Cervetto, J. Helbing, J. Bredenbeck, and P. Hamm, J. Chem. Phys. **121**, 5935 (2004).
10. K. J. Kubarych, M. Joffre, A. Moore, N. Belabas, and D. M. Jonas, Opt. Lett. **30**, 1228 (2005).
11. M. J. Nee, R. McCanne, K. J. Kubarych, and M. Joffre, Opt. Lett. **32**, 713 (2007).
12. M. Khalil, N. Demirdöven, and A. Tokmakoff, J. Phys. Chem. A **107**, 5258 (2003).
13. M. J. Nee, C. R. Baiz, J. M. Anna, R. McCanne, and K. J. Kubarych, J. Chem. Phys. **129**, 084503 (2008).
14. M. J. Tauber, R. A. Mathies, X. Y. Chen, and S. E. Bradforth, Rev. Sci. Instrum. **74**, 4958 (2003).
15. D. A. Steinhurst, A. P. Baronavski, and J. C. Owrutsky, Chem. Phys. Lett. **361**, 513 (2002).